Nonlinear Optical Spectroscopy on One-Dimensional Excitons in Silicon Polymer, Polysilane

T. Hasegawa, Y. Iwasa, H. Sunamura, and T. Koda
Department of Applied Physics, The University of Tokyo, Tokyo 113, Japan

Y. Tokura
Department of Physics, The University of Tokyo, Tokyo 113, Japan

H. Tachibana and M. Matsumoto
National Chemical Laboratory for Industry, Tsukuba 305, Japan

S. Abe
Electrotechnical Laboratory, Tsukuba 305, Japan
(Received 9 March 1992)

The modulus and phase of the complex third-order nonlinear optical (NLO) susceptibility $\tilde{\chi}^{(3)}(-3\omega;\omega,\omega,\omega)$ have been measured on an all-trans silicon polymer, poly(dihexylsilane), over a wide photon energy range. Several distinct structures observed in the $\tilde{\chi}^{(3)}$ spectra are in excellent agreement with the theoretical results of a one-dimensional (1D) exciton model. Important aspects of the 1D Wannier-like exciton structure in polysilanes are elucidated in relation to the NLO processes.

PACS numbers: 73.20.Dx, 42.70.Nq, 71.35.+z, 78.65.Hc

Much interest has been focused on the quasi-one-dimensional (1D) semiconductors. In σ-bonded inorganic semiconductors, nanoscopic structures called quantum wires are fabricated by elaborate techniques of crystal growth and microlithography [1]. Meanwhile, various organic polymers are synthesized to utilize the delocalized π-conjugated electronic states on the linear polymer chains [2]. In such quasi-1D inorganic as well as organic semiconductors, the lowest dipole-allowed exciton is predicted to have a very large binding energy and an unusually strong oscillator strength [3–5], due to the singular character of the 1D Coulomb potential for excitons [6]. This problem has attracted considerable interest from the viewpoint of solid-state physics, but the details remain unexplored as of yet. In this paper, we report the third-order nonlinear optical (NLO) spectra of a silicon polymer, polysilane, demonstrating that the characteristic features of quasi-1D (Wannier-like) excitons can be fully revealed by nonlinear optical spectroscopy.

Among the various kinds of polysilanes ($\{SiRR'\}$, R and R' being organic sidegroups) with different conformations [7], we have chosen poly(dihexylsilane) (PDHS; $R,R'=C_6H_{13}$) with an all-trans planar structure of σ-bonded Si chains (with a d_{2h} symmetry), which may be regarded as a model system of the 1D analog (or "an ultimate quantum wire") of a 3D silicon crystal. This polymer is predicted to have a direct gap between the σ-bond-like valence band and the σ^*-bond-like conduction band at the Γ point [8]. The sharp absorption peak at 3.30 eV is assigned to the lowest allowed ^1B_u exciton, while the two-photon absorption peak at 4.19 eV [9–11] is assigned to the second forbidden ^1A_g exciton. However, the whole profile of the 1D excitonic structure has not yet been disclosed.

To elucidate the quasi-1D excitonic structure in PDHS, we have undertaken extensive NLO spectroscopy over a wide photon energy range, as recently attempted on various π-conjugated polymers [12]. In the sample preparation, PDHS powders with molecular weight of about 2.44×10^5 were dissolved in heptane, and the solution was spin casted onto synthetic fused silica plates to form unoriented film samples. The films were dried at 380 K for 15 min and allowed to stand at room temperature overnight, before optical measurements.

In the measurements of $\tilde{\chi}^{(3)}(-3\omega;\omega,\omega,\omega)$ three kinds of tunable laser systems were used: a dye laser driven by a 15-ns-wide Xe-Cl excimer laser with use of thirteen kinds of dyes (Lambdachrome laser dyes) in the range from 2.15 to 1.20 eV (University of Tokyo), a tunable H_2:Raman laser pumped by another dye laser pumped by second-harmonic beams of a 5.5-ns-wide Nd:YAG laser in the range from 1.18 to 0.91 eV (RIKEN), and a difference frequency generator using a $LiNbO_3$ crystal coupled with a Nd:YAG laser and a dye laser in the range from 0.82 to 0.56 eV (NTT). By the combination of them, we were able to scan the pumping photon energy continuously from 2.15 to 0.56 eV. The laser beam was focused onto the sample, using a 10-cm-focal-length lens. The third-harmonic (TH) light from the sample was detected by a photomultiplier tube, and then processed by a boxcar averager. The dependence of the TH intensity on the cube of the fundamental laser power was carefully checked frequently to establish the limit of linearity between the output signal and the TH intensity. Samples were placed in a vacuum cell to avoid the air contribution to the observed TH intensities. All measurements were made at room temperature.

The dispersion of the modulus $|\chi^{(3)}|$ and that of the phase ϕ of the complex third-order NLO susceptibility $\tilde{\chi}^{(3)}=|\chi^{(3)}|e^{i\phi}$ provide crucial information on the multi-

photon resonant processes in PDHS, through the energy-dependent denominators $[E_i - nE - i\gamma_i]^{-1}$ $(n=3,2,1)$ [13]; E is the photon energy, and E_i and γ_i are the energy and the damping constant of a relevant level i, respectively. It is to be noted that, unlike the modulus $|\chi^{(3)}|$, the phase ϕ directly reflects the electronic structure, irrespective of the sample density. The experimental evaluation methods of the $|\chi^{(3)}|$ and ϕ values are described in detail in the literature [14–16], and we shall only mention here the following remarks: In the modulus measurements, all samples were prepared from the same solution under the same condition to keep the thickness constant (which was estimated to be about 0.15 μm). The internal attenuation of the TH fields was corrected by using the experimental absorption coefficient. (The effect of refractive index dispersion was not taken into account in the present approximation, since this effect does not significantly change the spectral shape of $\tilde{\chi}^{(3)}$.) In the phase measurement, the thickness of film was carefully adjusted in the range of about 0.03–0.15 μm, depending on the fundamental photon energy, by changing the polymer concentration in the spin-casted solution. This procedure was important to observe well-defined Maker fringes caused by the interference between the TH fields generated from the polymer film and from the silica plate. The modulus and phase values of PDHS were determined by using those values of silica as the standard. For this purpose, the values of $\chi^{(3)}$ and of the coherence length of silica were evaluated up to 2.2 eV using the measured index of refraction. The absolute values of $\chi^{(3)}$ were determined by extrapolating the reported value at 1.907 μm (0.650 eV) [17] by using the Miller rule.

The experimental results thus obtained are plotted in Fig. 1. These values represent $\tilde{\chi}^{(3)}_{1111}$ (1 denotes the coordinate fixed to the sample) which is the orientational average of $\gamma_{xxxx}(-3\omega;\omega,\omega,\omega)$ (x is the axis fixed to the polymer chain). The dotted lines represent the theoretical curves which will be described later. In the photon energy region above 2.0 eV, the laser beam caused serious degradation of the film. In the phase measurement, where sufficient laser power was required to observe the TH fields from both the thinner film and the silica substrate, reliable estimates of the phase values were not feasible in this region. In the modulus measurement, however, this effect could be eliminated by using thicker films for which sufficient TH intensities could be detected at lower laser powers.

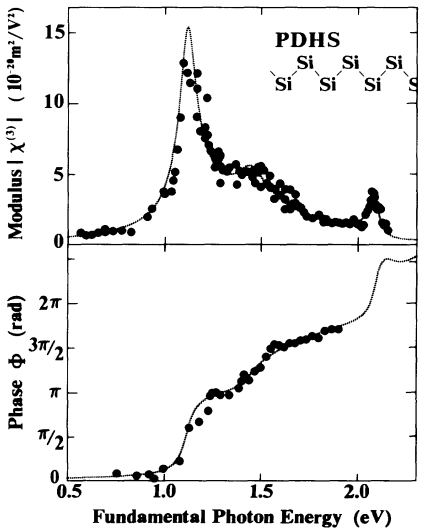

FIG. 1. Dispersion of modulus $|\chi^{(3)}|$ (upper) and phase ϕ (lower) for complex $\tilde{\chi}^{(3)}(-3\omega;\omega,\omega,\omega)=|\chi^{(3)}|e^{i\phi}$ of all-trans polysilane PDHS at room temperature. Experimental results (filled circles) are compared with theoretical spectra (dotted lines).

Several features are noticed in the experimental spectra shown in Fig. 1: The main peak in the $|\chi^{(3)}|$ spectrum at about 1.10 eV is accompanied by a sharp phase shift from 0 to π rad, crossing $\pi/2$ rad at the peak position. The second peak (or a shoulder) at around 1.50 eV is also accompanied by a steep variation of ϕ. A weak but distinct peak of $|\chi^{(3)}|$ is observed at about 2.10 eV. Of these features, the first peak has been attributed to the three-photon resonance to the lowest (^1B_u) exciton at around 3.30 eV, while the third peak to the two-photon resonance to the second (^1A_g) exciton at around 4.19 eV [18–20].

In Fig. 2, we replotted the $|\chi^{(3)}|$ spectrum against the fundamental photon energy ($\hbar\omega$), together with the

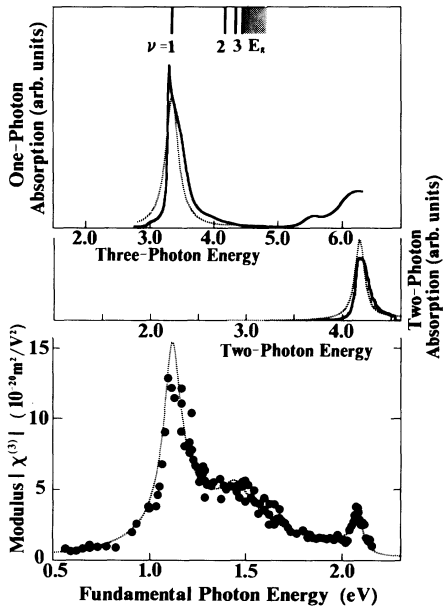

FIG. 2. Linear and third-order NLO spectra of all-trans polysilane PDHS; one-photon absorption (top), two-photon absorption (middle), and modulus $|\chi^{(3)}|$ spectra, all at room temperature. Note the change in the respective photon energy scales to demonstrate multiphoton resonance effect. Experimental and theoretical spectra are plotted by solid lines (or circles) and dotted lines, respectively. The calculated exciton level structure is shown at the top of the one-photon absorption spectrum.

one-photon absorption spectrum (top) and the two-photon absorption spectrum (middle), against the three-photon ($3\hbar\omega$) and the two-photon ($2\hbar\omega$) energies, respectively. The three-photon and two-photon resonance effects for the peaks at around 1.10 and 2.10 eV in the $|\chi^{(3)}|$ spectrum are evident from this plot, confirming the previous interpretation [18–20]. But the origin of the 1.50-eV peak is not obvious from the comparison of these spectra. Note the following peculiar features of this peak: The fairly steep variation of the phase observed around this energy indicates that a considerable resonance enhancement effect is involved in the NLO process, while there is no observable peak in the one-photon absorption spectrum. These features will be elucidated by the theoretical analysis described below.

In the theoretical calculation, an all-trans linear chain of Si atoms was modeled by a σ-conjugated 1D system of skeleton sp^3 electrons with intrinsically alternating transfer energies ($t_0 \pm \delta t$) [10,21] and long-range Coulomb interactions. For the latter, we assumed on-site electron repulsion U and intersite electron repulsion $e^2/\varepsilon R_{ij}$ screened by the dielectric constant ε, R_{ij} being the distance between the ith and jth orbitals in the chain [21]. Using this model, bound as well as unbound electron-hole states were calculated numerically for a finite chain of 500 atoms by using a standard method [22] diagonalizing the Hamiltonian within the subspace of single electron-hole excitations. Then, the $\tilde{\chi}^{(3)}$ spectrum was calculated using a standard formula [13] by carrying out summations over all the obtained states, taking damping constants γ_i into account [23].

After suitable parameter fitting, the theoretical curves (dotted lines) in Figs. 1 and 2 were obtained for $t_0 = 1.85$ eV, $\delta t = \frac{1}{3} t_0$, $U = 2.8 t_0$, and $\varepsilon = 5.5$ [24]. The damping constants γ_i were assumed to be 0.12 eV for the first allowed (1^1B_u, $v=1$ [25]) exciton transition, 0.06 eV for the next forbidden (2^1A_g, $v=2$) exciton transition, and 0.18 eV for all other allowed transitions. The agreement between the experimental and theoretical results is satisfactory, as seen in Figs. 1 and 2, supporting the present 1D exciton model. The calculated energies of $v=1,2,3$ excitons and the band gap E_g are shown at the top of the one-photon absorption spectrum in Fig. 2.

The comparison of experimental and theoretical results allows us to interpret the 1.50-eV peak in the $\tilde{\chi}^{(3)}$ spectra, left unclear in the preceding discussion, as being due to the significant contributions from the $v=3$ and higher states around E_g including unbound electron-hole states. In the one-photon process, the absorption intensity for the $v=i$ exciton is proportional to μ_{0i}^2, where μ_{0i} is the transition dipole moment $\mu_{0i} = \langle 0|\mu|i\rangle$ ($|0\rangle$ is the ground state). Hence, the relative absorption intensities for the $v=3$ and 1 excitons are given by the ratio $(\mu_{03}/\mu_{01})^2$. According to the calculation, this ratio is $(0.08)^2 \simeq 0.006$, in agreement with the theoretical prediction that the lowest exciton absorption becomes predominant in a 1D semiconductor [3–5]. In the third-order NLO process, on the other hand, the $\tilde{\chi}^{(3)}$ formula contains fourth-order terms like $\mu_{0i}\mu_{ij}\mu_{jk}\mu_{k0}$, where i,j,k represent the intermediate states in the NLO process. Accordingly, the predominant contributions to the three-photon resonance with the $v=3$ and $v=1$ excitons are proportional to $\mu_{01}\mu_{12}\mu_{23}\mu_{30}$ and $\mu_{01}^2\mu_{12}^2$, respectively. Their intensity ratio is approximately given by $\mu_{23}\mu_{30}/\mu_{01}\mu_{12} = (\mu_{23}/\mu_{21})(\mu_{03}/\mu_{01})$, which is calculated to be $2.8 \times 0.08 \simeq 0.22$. The larger contribution of the $v=3$ exciton in the third-order NLO response compared to the linear response is attributed to the fact $\mu_{23}/\mu_{21} \gg \mu_{03}/\mu_{01}$. (A similar mechanism is suggested [21] to be responsible for a structure in the electroabsorption spectrum of PDHS in the corresponding high-energy region [26].)

The 1D exciton structure in PDHS thus revealed is illustrated in Fig. 3. Here, we plotted the profiles of envelope functions for the $v=1$, 2, and 3 excitons against the electron-hole separation $x_e - x_h$ in units of the lattice constant a ($=2.0$ Å). The following interesting features are seen in this plot: First, the lowest ($v=1$) exciton is strongly localized within a few lattice constants, reflecting the 1D character of the potential (shown by a dashed curve). As a result, this exciton has a binding energy as large as 1.1 eV and a large transition dipole moment. Another notable feature is the shapes of the wave functions for the $v=2$ and 3 excitons. In an ideal 1D Coulomb potential, these two states are degenerate, both having a node at the origin [6]. In the present model, however, they split. But the separation is still relatively small (about 0.2 eV), so that even the $v=3$ exciton has a fairly small amplitude at the origin, and is delocalized over a few tens of lattice constants. Such 1D exciton features explain why the dipole moment μ_{03} is so small compared with μ_{01}, and why μ_{23} is so large compared with μ_{21}.

In conclusion, we have established a 1D Wannier-like exciton picture in PDHS, which is essential in interpret-

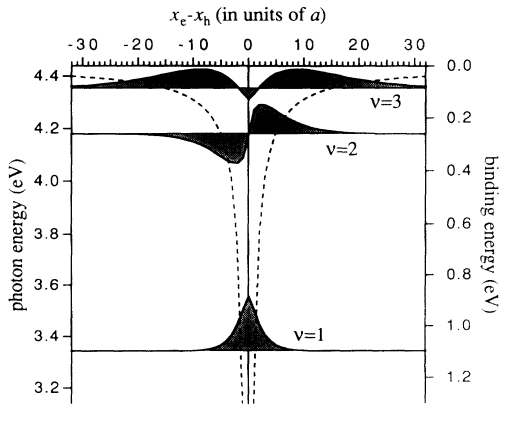

FIG. 3. 1D exciton structure calculated for all-trans polysilane PDHS. Exciton envelope functions (shaded solid curves) and model potential (dashed curve) are plotted against the electron-hole distance in units of the lattice constant a ($=2$ Å).

ing the NLO properties of this polymer. Such a solid-state physical approach is meaningful in the study of the microscopic mechanism of NLO processes in polysilanes, supplementing previous results of quantum chemical approaches [10,27].

The authors are grateful to Dr. H. Kobayashi and Dr. K. Kubodera (NTT Optoelectronics Laboratories) and to Dr. S. Wada, L. T. Thi, and Professor H. Tashiro (Laser Science Group, RIKEN, Institute of Physical and Chemical Research) for their experimental collaboration, and to Professor K. Miyano, Dr. S. Koshihara, and H. Kishida for helpful discussions. This work was supported in part by a Research-Grant-in-Aid from the Ministry of Education, Culture and Science in Japan, the Nissan Science Foundation, and the NEDO Foundation, Japan.

[1] For example, M. Kohl, D. Heitmann, P. Grambow, and K. Ploog, Phys. Rev. B **37**, 10927 (1988).

[2] For example, *Nonlinear Optical Effects in Organic Polymers*, edited by J. Messier, F. Kajzar, P. Prasad, and D. Ulrich (Kluwer Academic, Dordrecht, 1989).

[3] R. J. Elliot and R. Loudon, J. Phys. Chem. Solids **15**, 196 (1960).

[4] S. Abe, J. Phys. Soc. Jpn. **58**, 62 (1989).

[5] T. Ogawa and T. Takagahara, Phys. Rev. B **43**, 14325 (1991).

[6] R. Loudon, Am. J. Phys. **27**, 649 (1959).

[7] R. D. Miller and J. Michl, Chem. Rev. **89**, 1359 (1989).

[8] K. Takeda and K. Shiraishi, Phys. Rev. B **39**, 11028 (1989).

[9] J. R. G. Thorne, Y. Ohsako, J. M. Zeigler, and R. M. Hochstrasser, Chem. Phys. Lett. **162**, 455 (1989).

[10] Z. G. Soos and R. G. Kepler, Phys. Rev. B **43**, 11908 (1991).

[11] Y. Moritomo, Y. Tokura, H. Tachibana, Y. Kawabata, and R. D. Miller, Phys. Rev. B **43**, 14746 (1991).

[12] For examples, F. Kajzar and J. Messier, Thin Solid Films **132**, 11 (1985); T. Kanetake *et al.*, Appl. Phys. Lett. **54**, 2287 (1989); W.-S. Fann *et al.*, Phys. Rev. Lett. **62**, 1492 (1989); T. Hasegawa *et al.*, Chem. Phys. Lett. **171**, 239 (1990); W. E. Torruellas *et al.*, Chem. Phys. Lett. **30**, 11 (1990); J. B. van Beek *et al.*, J. Chem. Phys. **95**, 239 (1991).

[13] B. J. Orr and J. F. Ward, Mol. Phys. **20**, 513 (1971).

[14] F. Kajzar, J. Messier, and C. Rosilio, J. Appl. Phys. **60**, 3040 (1986).

[15] D. Neher, A. Wolf, C. Bubeck, and G. Wegner, Chem. Phys. Lett. **163**, 116 (1989).

[16] T. Hasegawa, K. Ishikawa, T. Koda, K. Takeda, H. Kobayashi, and K. Kubodera, Synth. Met. (to be published).

[17] F. Kajzar and J. Messier, Phys. Rev. A **32**, 2352 (1985).

[18] J. R. G. Thorne, J. M. Zeigler, and R. M. Hochstrasser, in *Long Scale Molecular Systems*, edited by W. Gans, NATO ASI Ser. (Plenum, New York, 1991).

[19] T. Hasegawa, Y. Iwasa, H. Kishida, T. Koda, Y. Tokura, H. Tachibana, and Y. Kawabata, Phys. Rev. B **45**, 6317 (1992).

[20] Y. Iwasa, T. Hasegawa, T. Koda, Y. Tokura, H. Tachibana, and Y. Kawabata, Synth. Met. (to be published).

[21] S. Abe, M. Schreiber, and W.-P. Su, Chem. Phys. Lett. (to be published).

[22] R. S. Knox, *Theory of Excitons* (Academic, New York, 1963).

[23] S. Abe, J. Yu, and W. P. Su, Phys. Rev. B **45**, 8264 (1992).

[24] U was chosen such that $U=2V_1$, where V_1 denotes the nearest-neighbor Coulomb repulsion, $V_1=e^2/\varepsilon R_{i,i+1}$. The values of t_0 and δt are reasonable compared with the band structure obtained by a first-principles study [8].

[25] Excitons are denoted by $\nu=1,2,3,\ldots$, in sequence of energy. These states correspond to the $n=0$, 1 (odd), 1 (even), . . . states, respectively, of a 1D hydrogen atom with the energy of $E_n=-R_d/n^2$, where R_d is the Rydberg energy [6].

[26] H. Tachibana, Y. Kawabata, S. Koshihara, and Y. Tokura, Solid State Commun. **75**, 5 (1990).

[27] B. Kirtman and M. Hasan, J. Chem. Phys. **96**, 470 (1992).

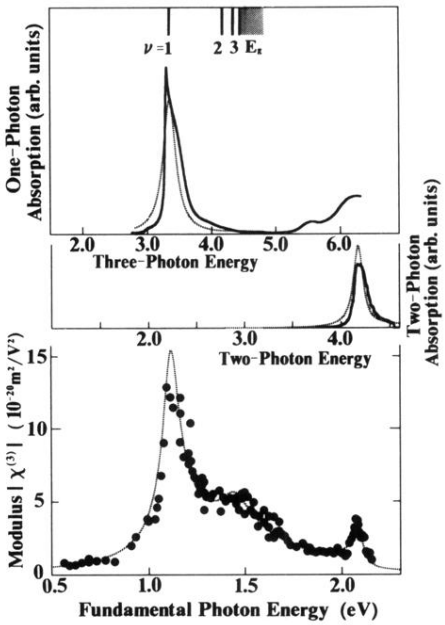

FIG. 2. Linear and third-order NLO spectra of all-trans polysilane PDHS; one-photon absorption (top), two-photon absorption (middle), and modulus $|\chi^{(3)}|$ spectra, all at room temperature. Note the change in the respective photon energy scales to demonstrate multiphoton resonance effect. Experimental and theoretical spectra are plotted by solid lines (or circles) and dotted lines, respectively. The calculated exciton level structure is shown at the top of the one-photon absorption spectrum.

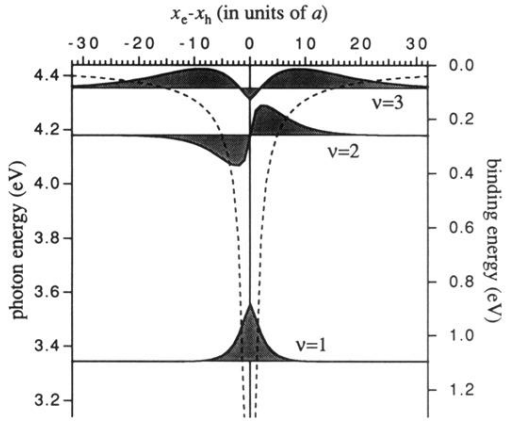

FIG. 3. 1D exciton structure calculated for all-trans polysilane PDHS. Exciton envelope functions (shaded solid curves) and model potential (dashed curve) are plotted against the electron-hole distance in units of the lattice constant a (=2 Å).